J. Electroanal. Chem., 281 (1990) 257–272
Elsevier Sequoia S.A., Lausanne – Printed in The Netherlands

Kinetics of CO_2 electroadsorption on electrodispersed platinum electrodes in acid solutions

M.L. Marcos, J. González-Velasco, J.M. Vara, M.C. Giordano *, and A.J. Arvia ***

Departamento de Electroquímica, Universidad Autónoma de Madrid, Canto Blanco, Madrid (Spain)

(Received 30 June 1989; in revised form 14 November 1989)

ABSTRACT

The kinetics of CO_2 electroadsorption on electrodispersed Pt electrodes have been investigated in different acid electrolytes. The kinetic data obtained at different adsorption potentials, adsorption times and CO_2 concentrations in solution have been interpreted in terms of two complex reaction mechanisms involving the formation of strongly and weakly bound reduced CO_2 adsorbates through reactions involving s-H and w-H adatoms, respectively, and carbon dioxide. The reaction mechanism between H adatoms and CO_2 implies the initial electroadsorption of H atoms, the transport of CO_2 from the bulk of the solution to the reaction interface, and the formation of the reduced CO_2 adsorbate. Under certain conditions, particularly when s-H adatoms are involved, the entire reaction approaches mass transport rate control. Conversely, the reaction between w-H adatoms and CO_2 appears as a rather slow process.

INTRODUCTION

The electrochemical reduction of CO_2 has received particular attention in recent years from the standpoint of electrochemical energy conversion by using organic fuels and as a specially attractive reaction for electrosynthesis processes [1–3]. It is well known that CO_2-containing adsorbates can be formed electrochemically on the surface of those metals which can electroadsorb H atoms, such as Pt, Rh, Pd and activated Au [4–20]. The electrochemical oxidation of reduced CO_2 adsorbate either voltammetrically or potentiostatically has been investigated on bright and platinized Pt [4–13], and more recently on electrodispersed Pt electrodes, i.e. rough Pt electrodes with a definite structure [21,22]. In contrast, much less is known about the kinetics of the adsorbate electroformation [5,11–13], an aspect of the entire

* Visiting Professors from INIFTA, Universidad Nacional de La Plata, La Plata, Argentina.
** Deceased.

0022-0728/90/$03.50

electrochemical reaction which deserves further study to reach a better knowledge of the characteristics of the electroadsorbate.

The reduced CO_2 species on Pt was associated with a COOH-type radical on the Pt surface which was formed according to either a second order reaction in the range 0.05–0.15 V, or a first order reaction with respect to adsorbed H atoms in the range 0.20–0.25 V [11–13]. In the former case, the H adatom + CO_2 molecule step becomes rate determining, whereas for the latter the probable rate determining step was associated with the reorientation of the adsorbed intermediate [13].

The distinct kinetic behaviour of CO_2 adsorption on Pt electrodes was interpreted as a change in the reaction pathway without considering the possibility that different adsorbates could result, depending on the involvement of either strongly or weakly bound H-adatoms as reactants. Recent electrochemical data on reduced CO_2 electrooxidation provided clear information about the occurrence of distinguishable reduced CO_2 adsorbates, a fact which encourages further investigation of the kinetics and mechanism of electroadsorbate formation proper.

In the present work, the kinetics of CO_2 electroadsorption on electrodispersed Pt electrodes are studied in different acid solutions in order to confirm the probable mechanism of reduced CO_2 adsorbate formation. This type of electrode exhibits a reproducible behaviour which is determined by regular domains of a sticking-cluster-like topography associated with a brush-like structure, as has been concluded from scanning tunelling microscopy at the nm level combined with scanning electron microscopy imaging [23,24]. One of the advantages of electrodispersed Pt electrodes is the possibility that different roughness characteristics can be developed by keeping the morphology of the metal overlayer nearly constant.

EXPERIMENTAL

Most of the experimental setup, i.e. the electrolysis cell and the electronic circuitry, were the same as already described in previous publications [21,22]. Electrodispersed Pt working electrodes with roughness factors, R, up to 70 were used. The preparation and surface treatment of the working electrodes as well as the definition of R and its determination have been described extensively elsewhere [21,22,25]. Two groups (I and II) of electrolyte solutions were employed; group I included solutions consisting of different CO_2 saturated acidic solutions, namely, 0.05 M $HClO_4$, 1 M $HClO_4$, 0.5 M H_2SO_4, and 1 M H_3PO_4, and group II, solutions involving 0.5 M H_2SO_4 with different CO_2 concentrations. Runs were made at 25 °C with O_2-free electrolyte solutions.

Operating conditions with group I solutions

Two electrodispersed Pt electrodes with initial geometric areas of 0.114 and 0.170 cm^2, and two different roughness factors, $R = 70$ and $R = 21$, were used. The potential programme applied to the working electrode comprised an initial potential step at 1.4 V lasting for several minutes for cleaning, followed by a potential jump to the adsorption potential, E_{ad}, which was held for an adsorption time t_{ad}. Then

the electrochemical experiment was continued in one of the following two ways: (a) the potential was stepped to a lower limit, $E_{s,c} = 0.05$ V, and subsequently, the potential was swept at 0.005 V/s in the positive direction; (b) the potential was swept at 0.005 V/s in the positive direction immediately after electroadsorbate formation at E_{ad} had occurred.

Operating conditions with group II solutions

The electrodispersed Pt electrode used in this case had an initial geometric area of 0.135 cm^2 and $R = 26$. The CO_2 concentration in solution was changed from 2.5×10^{-3} M to 2.5×10^{-2} M by adding the right amount of Na_2CO_3 solution of known concentration to a nitrogen saturated H_2SO_4 solution in order to reach the preset final CO_2 concentration in 0.5 M H_2SO_4. The CO_2 saturation concentration in this solution at 25 °C is ca. 2.5×10^{-2} M [26]. The potential programme employed in this case is similar to that described for procedure (a) in the preceding paragraph, but the potential sweep rate was set to 0.05 V/s in order to avoid large changes in the CO_2 concentration during the experiment. Then, $\theta_{CO_2,r}$, the degree of surface coverage by reduced CO_2, was taken as $1 - \theta_H$, where θ_H, the degree of H atom surface coverage was measured as the ratio between Q_H and Q_H°, the H adatom voltammetric electrooxidation charge density in the presence and in the absence of CO_2 in solution, respectively, ($\theta_H = Q_H/Q_H^\circ$).

RESULTS AND INTERPRETATION

Typical electrooxidation voltammograms for reduced CO_2 adsorbates at electrodispersed Pt electrodes obtained according to the operating conditions for group

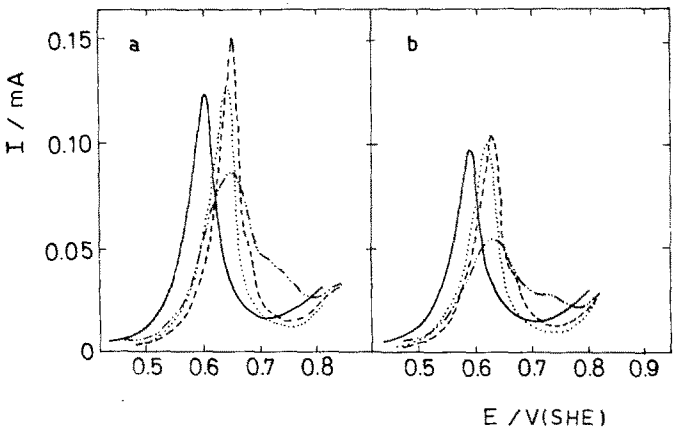

Fig. 1. Electrooxidation potentiodynamic profiles run for $E_{ad} = 0.115$ V at 0.005 V/s and different t_{ad}/s = (a) 300, (b) 60. Geometric Pt electrode area 0.114 cm^2. $R = 70$. The electrolyte solutions are under CO_2 saturation. 25 °C. Electrolyte: (———) 0.05 M $HClO_4$, (— — —) 1.00 M $HClO_4$, (· · · · · ·) 0.50 M H_2SO_4, (–·–·–·–) 1.00 M H_3PO_4.

I solutions at constant E_{ad}, two values of t_{ad}, and 0.05 V/s are depicted in Fig. 1. A rather symmetric anodic current peak at ca. 0.6 V is obtained in 0.05 M $HClO_4$, but the peak potential shifts positively with either a shoulder or a second partially overlapping anodic current peak in going from 0.05 M $HClO_4$ to 1 M $HClO_4$, 0.5 M H_2SO_4 and 1 M H_3PO_4. These results confirm the complexity of the electrooxidation of reduced CO_2 adsorbates and the influence of anions on the process, as has been reported previously [17,18,22]. It should be noted that the data obtained for electrodispersed Pt electrodes are very reproducible, and in this case, the interference of possible adsorbable impurities in solution can be considered as negligible, as for large surface area Pt electrodes.

From $Q^a_{CO_2r}$, the voltammetric electrooxidation (stripping) charge related to the reduced CO_2 adsorbates, and its dependence on t_{ad}, E_{ad} and CO_2 concentration in the various acidic solutions, one can obtain information about the adsorption kinetics of CO_2 yielding reduced CO_2 adsorbates on electrodispersed Pt electrodes. For this case, since the adsorption data are derived from the stripping voltammograms, the true adsorption time, t_{ad}, corresponds to the sum of the time spent at E_{ad} and the time used up to sweep the potential from E_{ad} up to 0.6 V, a potential

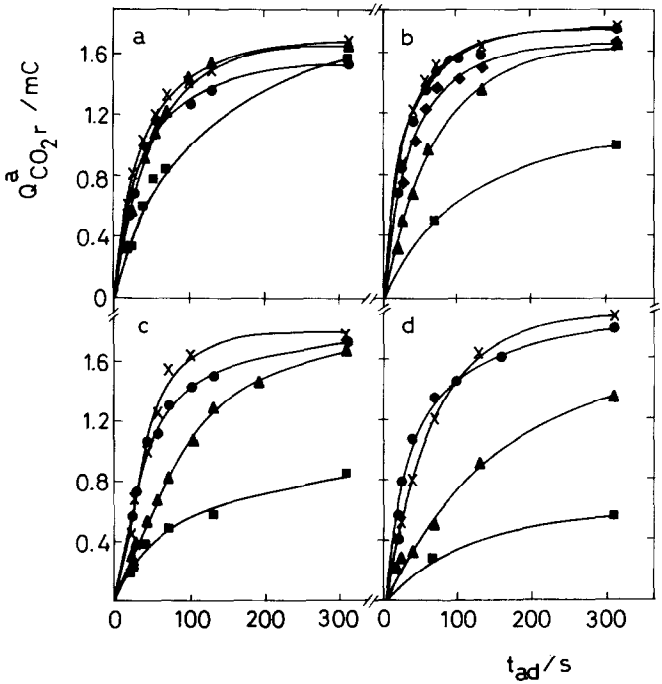

Fig. 2. $Q^a_{CO_2r}$ (voltammetric stripping charge) vs. t_{ad} plots. Data obtained at different E_{ad} in (a) 1 M $HClO_4$; (b) 0.05 M $HClO_4$; (c) 0.5 M H_2SO_4; (d) 1 M H_3PO_4. Geometric Pt electrode area 0.114 cm^2. $R = 70$; 25 °C. E_{ad}/V: (◆) 0.015, (●) 0.065, (×) 0.115, (▲) 0.165, (■) 0.215.

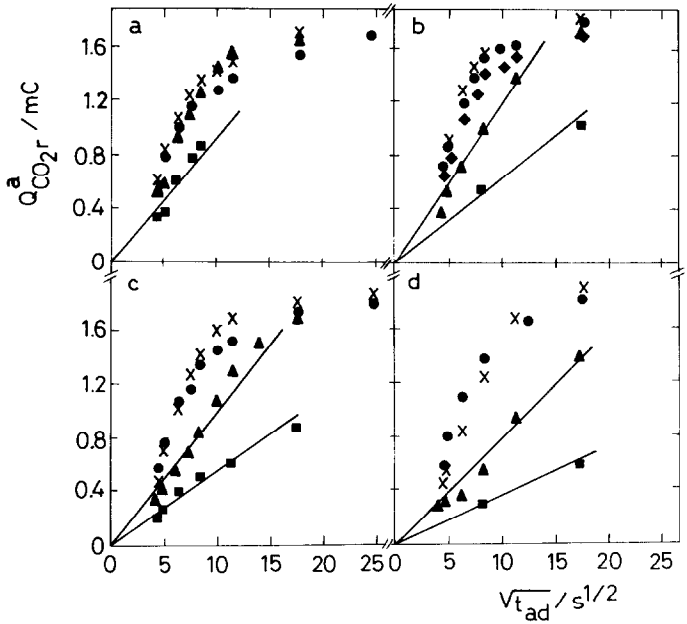

Fig. 3. $Q^a_{CO_2r}$ vs. $t_{ad}^{1/2}$ plots. Data obtained at different E_{ad} in (a) 1 M $HClO_4$; (b) 0.05 M $HClO_4$; (c) 0.5 M H_2SO_4; (d) 1 M H_3PO_4. Geometric Pt electrode area 0.114 cm^2. $R = 70$. 25 °C. E_{ad} as in Fig. 2.

value during stripping where it is supposed that the H atom concentration on the Pt surface becomes sufficiently low to contribute to the formation of reduced CO_2 adsorbates.

The $Q^a_{CO_2r}$ vs. t_{ad} plots (Figs. 2a–d) resulting for the different solutions exhibit several interesting features. In general, when E_{ad} is smaller than approximately 0.12 V, these plots are coincident, and as t_{ad} increases they attain a maximum limiting charge density value ($Q^a_{CO_2}$) = 17 ± 1.5 mC/cm^2 geometric area. Conversely, for E_{ad} greater than 0.12 V, the $Q^a_{CO_2r}$ vs. t_{ad} plots as well as the limiting ($Q^a_{CO_2}$) values show a clear dependence on E_{ad}. Therefore, from these plots one can conclude that there are at least two different types of kinetic behaviour related to the electroformation of reduced CO_2 adsorbate, depending on whether the H atom surface coverage is large or small. Otherwise, when $Q^a_{CO_2r}$ is plotted vs. $t_{ad}^{1/2}$ (Fig. 3), linear relationships can be observed only for those adsorption processes taking place at E_{ad} greater than 0.12 V and t_{ad} lower than 200 s. No reasonably linear portions can be drawn for the $Q^a_{CO_2r}$ vs. $t_{ad}^{1/2}$ plots resulting for E_{ad} lower than 0.12 V.

It is interesting to note that the transition between the two different types of kinetic behaviour which are observed at well defined E_{ad} potential ranges, can be correlated with the change in the H adatom charge vs. potential relationships resulting from the blanks (Figs. 4a–d). From the θ_H vs. E plots, it is possible to estimate θ^e_H, the equilibrium values of θ_H at different applied potentials, including $E = E_{ad}$. These data show that one of the types of CO_2 adsorption kinetics

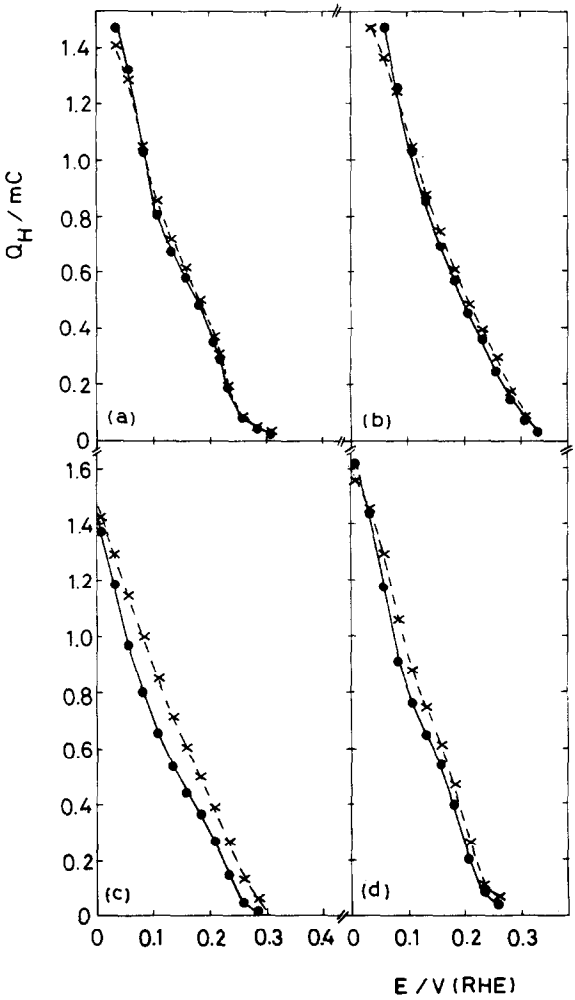

Fig. 4. Q_H vs. E plots obtained from voltammetric electroadsorptions and electrodesorption in: (a) 0.5 M H_2SO_4, (b) 1 M $HClO_4$, (c) 0.05 M $HClO_4$, (d) 1 M H_3PO_4. Geometric electrode area 0.114 cm^2. R = 70. 25 °C. (●) Adsorption, (×) desorption.

corresponds to the potential range of weakly adsorbed H atoms ($E_{ad} < 0.12$ V), whereas the other one is observed in the potential range of strongly bound H atoms ($E_{ad} > 0.12$ V). Accordingly, for E_{ad} values located in the potential range of strongly bound H atoms, the initial slope of the $Q^a_{CO_2r}$ vs. t_{ad} plots (Fig. 2) increases with the amount of that kind of H adatom present on the Pt surface at E_{ad}. In this case, first order kinetics with respect to the H adatom concentration at the Pt surface are apparently obeyed. These results suggest that, in the adsorption of CO_2 on Pt, at least two distinguishable reduced CO_2 adsorbates are produced, one

in the 0–0.12 V range, and the other in the 0.12–0.35 V range. In order to identify the type of H adatom involved in each reaction it is interesting to consider data resulting from voltammetric runs with solutions of different CO_2 concentration.

The voltammograms run according to the operating conditions described for group II solutions at 0.05 V/s and three different t_{ad} values (Figs. 5a–c), show that

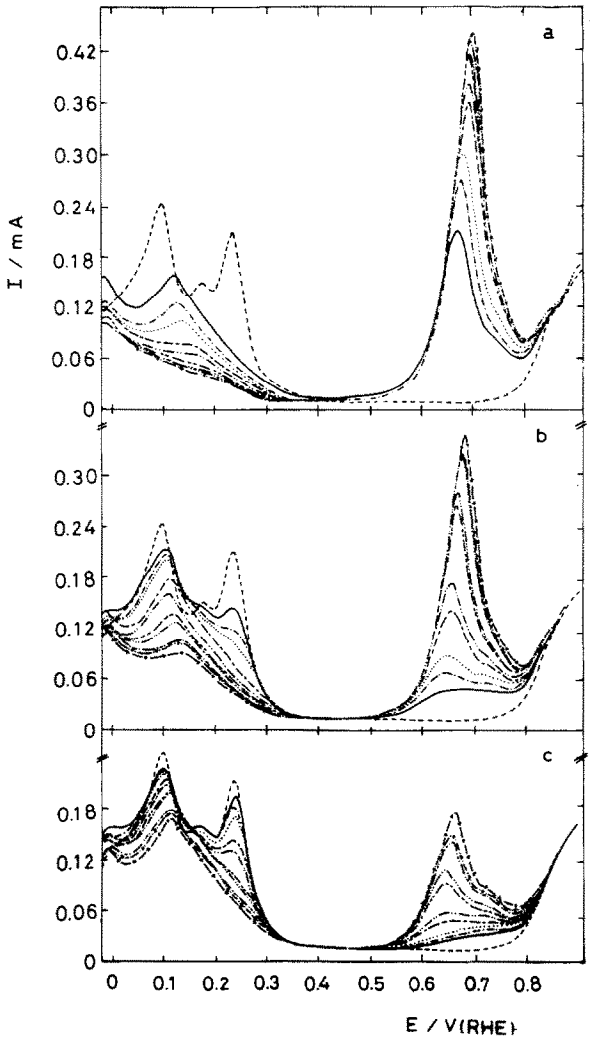

Fig. 5. Electrooxidation potentiodynamic profiles run from $E_c = -0.02$ V to $E_a = 0.9$ V at 0.05 V/s in 0.5 M H_2SO_4 containing different CO_2 concentrations. $E_{ad} = 0.115$ V and t_{ad}/s: (a) 300, (b) 60, (c) 15. Geometric Pt electrode area 0.135 cm^2. $R = 26$. 25 °C. c_{CO_2}/M: (- - - - - -) 0 (blank), (———) 0.0025, (– · – · –) 0.00375, (· · · · · ·) 0.005, (— · ——) 0.0075, (– · · – · · –) 0.01, (— — —) 0.0125, (– · · · –) 0.015, (– · · · –) 0.0175, (– · × · –) 0.02, (– + – + –) 0.025.

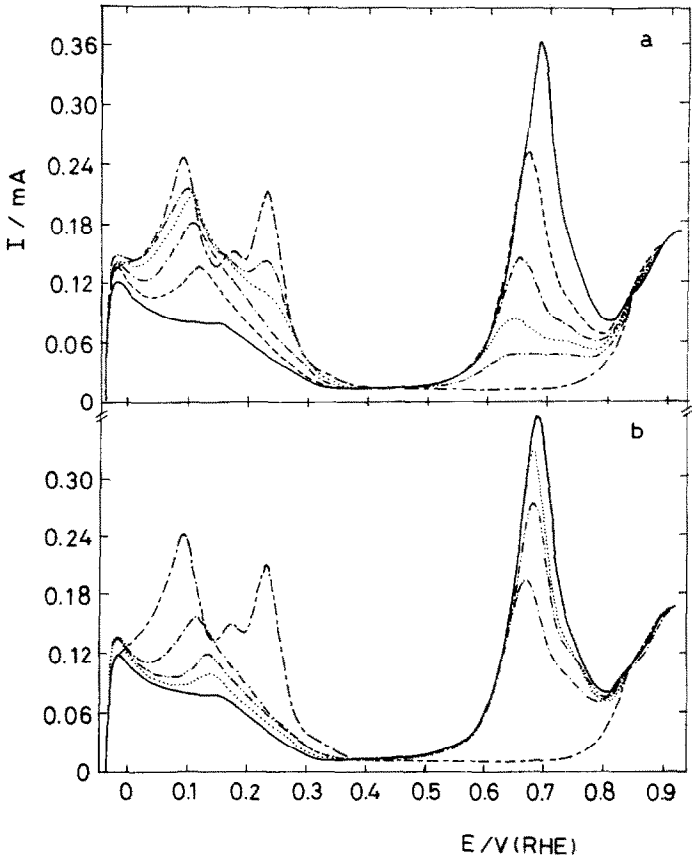

Fig. 6. Electrooxidation potentiodynamic profiles run at 0.05 V/s in 0.5 M $H_2SO_4 + 7.5 \times 10^{-3}$ M CO_2 with different t_{ad} (a) and E_{ad} (b). Geometric Pt electrode area 0.135 cm^2. R = 26. 25 °C. (a) E_{ad} = 0.115 V; c_{CO_2} = 0.0075 M. (——·——) Blank (c_{CO_2} = 0). t_{ad}/s: (———) 300, (- - - - -) 120, (–·–·–) 60, (·····) 30, (–··–··–) 15. (b) t_{ad} = 300 s; c_{CO_2} = 0.0075 M. E_{ad}/V: (–··–··–) 0.015, (·····) 0.065, (———) 0.115, (–·–·–) 0.165.

as the CO_2 concentration in solution increases, a sharper and better defined reduced CO_2 electrooxidation current peak is obtained. Consequently, the total H atom electrodesorption charge density, Q_H^a, decreases, particularly because the contribution of strongly bound H adatoms decreases. In addition one observes a shift of the peak potential related to the electrodesorption of weakly bound H adatoms towards more positive values as either the CO_2 concentration or t_{ad} increases (Fig. 6a). Similar effects can be obtained by changing E_{ad} (Fig. 6b), but in this case it is worthwhile to note that the maximum value for θ_{CO_2r} is found when E_{ad} = 0.115 V, as reported previously [11,13]. Under this condition the value of Q_H^a corresponds to about one half the maximum value of $(Q_{CO_2r}^a)_0$.

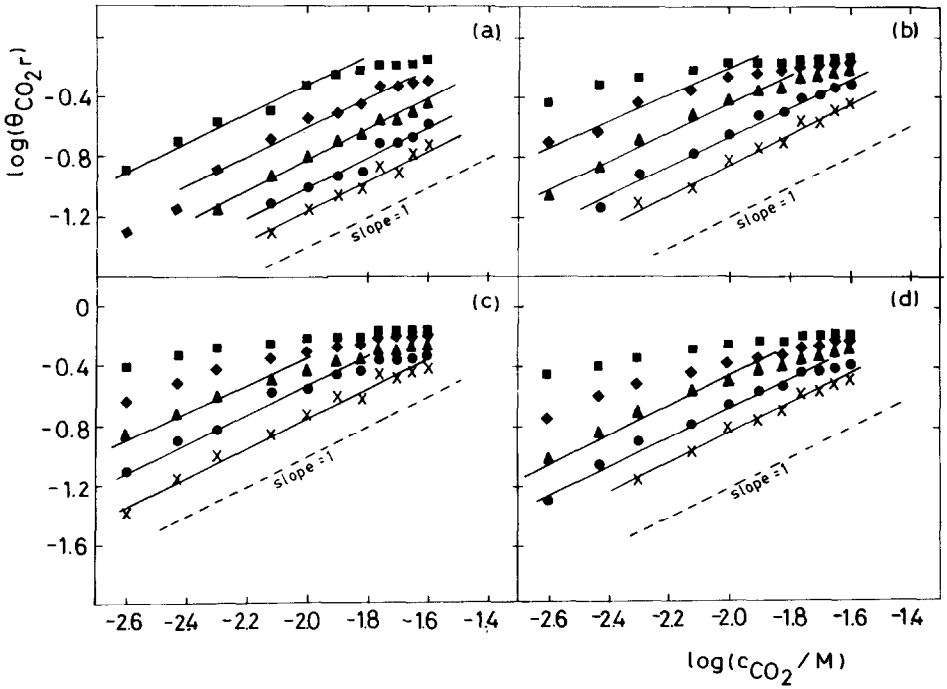

Fig. 7. Log θ_{CO_2r} vs. log c_{CO_2} plots for different E_{ad} and t_{ad}. 0.5 M H_2SO_4. Geometric Pt electrode area 0.135 cm^2. R = 26. 25 °C. E_{ad}/V: (a) 0.165, (b) 0.115, (c) 0.065, (d) 0.015. t_{ad}/s: (×) 15, (●) 30, (▲) 60, (■) 120, (◆) 300.

On the other hand, for the entire range of E_{ad}, but for $t_{ad} < 60$ s and at low CO_2 concentration in solution, the values of θ_{CO_2r} fit a linear dependence on the CO_2 concentration in solution, which can be seen when the data are plotted as log θ_{CO_2r} vs. log c_{CO_2} for different E_{ad} and t_{ad} values (Fig. 7). Furthermore, for $E_{ad} = 0.015$ V, on increasing both the CO_2 concentration in solution and t_{ad}, the limiting value of $(\theta_{CO_2r})_0$ is attained more easily, i.e. the slope $\Delta \log \theta_{CO_2r}/\Delta \log c_{CO_2}$ approaches zero. In general, the more extended linear log θ_{CO_2r} vs. log c_{CO_2} plots occur when the value of θ_H becomes lower than 0.5, that is, when the strongly bound H adatoms are involved in the reaction. Therefore, it appears that there is a change in the kinetics of CO_2 electroadsorption as one moves from an initial fast reaction involving predominantly strongly bound H adatoms, to a final slow reaction where the weakly bound H adatoms become the adsorbed reactants.

DISCUSSION

CO_2 adsorption on electrodispersed Pt in acid solutions, as already established for smooth and platinized Pt [4,6,7,9], requires the presence of H adatoms on the metal surface. The present results show that the electroadsorption of CO_2 involving

strongly bound H adatoms becomes faster than the electroadsorption of CO_2 through weakly bound H adatoms. In agreement with previously reported data for platinized Pt in 0.5 M H_2SO_4 [6], the overall reduced CO_2 electrooxidation reaction comprises a maximum charge density value slightly smaller than that expected for the H adatom monolayer.

On the other hand, the voltammetric data provide a clear indication that different reduced CO_2 adsorbates are produced depending on whether the electroadsorption reaction at E_{ad} takes place in the strongly or weakly bound H adatoms potential range, including as an additional variable the electroadsorption time. Furthermore, it is interesting to note that as the CO_2 adsorption takes place, the electrochemical characteristics of the H adatoms remaining unreactive on the Pt surface change rather drastically, as can be seen through the corresponding H adatom electrodesorption voltammograms. This effect is probably the result of a decrease in the local interaction energy (repulsive) among the remaining unreactive H adatoms as the adsorption of CO_2 proceeds. Finally, one can also note that the adsorption of CO_2 is only slightly sensitive to the electrolyte composition, in contrast to those processes related to the electrooxidation of the reduced CO_2 adsorbates [17,18,22]. By keeping these premises in mind, the interpretation of the kinetics of CO_2 electroadsorption on electrodispersed Pt in acid solutions can be approached in a way rather different from that advanced earlier for smooth and platinized Pt [11–13], although sufficiently general to embrace results obtained with any type of Pt electrode.

The formation of reduced CO_2 adsorbates can be put forward in terms of two similar reaction schemes comprising three steps, which, for a negative going linear potential sweep, can be written as follows:

Scheme I:

$$H^+(sol) + s\text{-}Pt(e^-) = (s\text{-}H)Pt \qquad (I\text{-}1)$$

$$CO_2(sol) = CO_2(elec) \qquad (2)$$

$$(s\text{-}H)Pt + CO_2(elec) = (s\text{-}CO_2r)Pt \qquad (I\text{-}3)$$

and

Scheme II:

$$H^+(sol) + w\text{-}Pt(e^-) = (w\text{-}H)Pt \qquad (II\text{-}1)$$

$$CO_2(sol) = CO_2(elec) \qquad (2)$$

$$(w\text{-}H)Pt + CO_2(elec) = (w\text{-}CO_2r)Pt \qquad (II\text{-}3)$$

Steps (I-1) and (II-1) indicate the reversible strongly (s) and weakly bound (w) H electrosorption reactions [26], taking place in the 0.15–0.30 V and 0.0–0.15 V ranges, respectively; s-Pt and w-Pt denote sites for strongly and weakly adsorbed H adatoms on the Pt surface. Therefore, $\theta_{s\text{-}H}$ and $\theta_{w\text{-}H}$, the degree of surface coverage by either s-H or w-H adatoms, respectively, depend on E_{ad}, the adsorption potential

value. Step (2) corresponds to the transport of CO_2 from the bulk of the solution, CO_2(sol), to the vicinity of the electrode surface, CO_2(elec); and steps (I-3) and (II-3) — depending on whether s-H or w-H atoms participate as one of the reactants — correspond to the adsorption of CO_2 proper, that is, the formation of strongly and weakly bound reduced CO_2 adsorbates, respectively. The probable structure of these adsorbates has already been discussed elsewhere [6,9,10,21]. The polycrystalline nature of electrodispersed Pt, as deduced from the intensity of the H atom electroadsorption–electrodesorption main voltammetric peaks, is consistent with a distribution of adsorption sites comprising about 50% s-Pt and 50% w-Pt sites. This conclusion is sustained by X-ray diffractometry, and voltammetric data combined with STM imaging of different preferred crystalline oriented and single crystal Pt electrodes [23–25,27–31].

Analysis of scheme I

Let us consider reaction scheme I and let us assume that quasi-stationary conditions for CO_2r electroadsorption are approached at low potentiodynamic sweep rates. Then, for the reaction taking place in the 0.15–0.35 V range (s-H adatom potential range) it follows that:

$$dc_{CO_2}(\text{elec})/dt_{ad} = \vec{k}_2 c_{CO_2}(\text{sol}) - \overleftarrow{k}_2 c_{CO_2}(\text{elec}) - \vec{k}'_{\text{I-3}} c_{CO_2}(\text{elec})\theta_{\text{s-H}} + \vec{k}'_{\text{I-3}}\theta_{\text{s-CO}_2\text{r}} = 0 \tag{4}$$

where k_i denotes the specific rate constant of the ith step ($i = 2$ and I-3) in the forward ($\rightarrow$) or backward ($\leftarrow$) directions, the k'_is are apparent rate constants, and $\theta_{\text{s-CO}_2\text{r}}$ stands for the degree of surface coverage by the strongly bound reduced CO_2 adsorbate. From eqn. (4) one obtains:

$$c_{CO_2}(\text{elec}) = \frac{\vec{k}_2 c_{CO_2}(\text{sol}) + \overleftarrow{k}'_{\text{I-3}}\theta_{\text{s-CO}_2\text{r}}}{\overleftarrow{k}_2 + \vec{k}'_{\text{I-3}}\theta_{\text{s-H}}} \tag{5}$$

Hence, $\vec{v}_{\text{I-3}}$, the rate of reaction (I-3) in the forward direction, is given by the expression:

$$\vec{v}_{\text{I-3}} = \frac{\vec{k}'_{\text{I-3}}\theta_{\text{s-H}}\left(\vec{k}_2 c_{CO_2}(\text{sol}) + \overleftarrow{k}'_{\text{I-3}}\theta_{\text{s-CO}_2\text{r}}\right)}{\overleftarrow{k}_2 + \vec{k}'_{\text{I-3}}\theta_{\text{s-H}}} \tag{6}$$

For this reaction scheme in the quasi-stationary state, the following conditions can be approached: $\overleftarrow{k}'_{\text{I-3}}\theta_{\text{s-CO}_2\text{r}} \ll \vec{k}_2 c_{CO_2}(\text{sol})$, and $\overleftarrow{k}_2 \ll \vec{k}'_{\text{I-3}}\theta_{\text{s-H}}$. In this case, it follows that

$$\vec{v}_{\text{I-3}} = \vec{k}_2 c_{CO_2}(\text{sol}) \tag{7}$$

Equation (7) predicts a first order dependence of the rate of formation of the reduced CO_2 adsorbate on CO_2 concentration in solution. This situation is better approached in the s-H-adatom potential range where step (I-3) behaves as a fast

step, as can be seen immediately from the voltammograms run at a constant E_{ad} and different t_{ad} values (Fig. 6a).

Another mechanistic approach can be made by starting from the first electron transfer step, which takes place under Langmuir adsorption conditions for s-H adatoms. Thus, the expression for $\theta_{s\text{-}H}$ is given by the equation:

$$\theta_{s\text{-}H} = 2\left[\frac{K_{s\text{-}H}c_{H^+}\exp(-F(E_{ad}-E^{p}_{s\text{-}H})/RT)}{1+K_{s\text{-}H}c_{H^+}\exp(-F(E_{ad}-E^{p}_{s\text{-}H})/RT)}\right] \tag{8}$$

where $k_{s\text{-}H} = \vec{k}_{I\text{-}1}/\overleftarrow{k}_{I\text{-}1}$, $E^{p}_{s\text{-}H}$ is the potential of the s-H adatom's reversible electrosorption voltammetric peak, and c_{H^+} is the hydrogen ion concentration in solution. Accordingly, at each E_{ad}, definite values of $\theta_{s\text{-}H}$ are obtained. The rate equation for formation of the s-CO_2r adsorbate can be written as follows:

$$\vec{v}_{I\text{-}3} = \vec{k}'_{I\text{-}3}\theta_{s\text{-}H}c_{CO_2}(\text{elec}) \tag{9}$$

Then, if one assumes that $c_{CO_2}(\text{elec}) \approx c_{CO_2}(\text{sol})$, the kinetics of the process should depend exclusively on the H adatom adsorption isotherm. Under this condition, considering that $\vec{v}_{I\text{-}3} \approx -(d\theta_{s\text{-}H}/dt_{ad}) = +(d\theta_{CO_2r}/dt_{ad})$, integration of eqn. (9) at a constant E_{ad} gives

$$-\ln\theta_{s\text{-}H} + \ln\theta^{\circ}_{s\text{-}H} = k'_{I\text{-}3}Fc_{CO_2}(\text{sol})t_{ad}/Q^{a}_{s\text{-}H} \tag{10}$$

where $Q^{a}_{s\text{-}H}$ is the maximum s-H adatom charge density attained at E_{ad}. Then, taking into account that CO_2 adsorbates are anchored through adsorbed H atoms, ($\theta_{s\text{-}H} + \theta_{CO_2r} = \text{const.}$), one can write:

$$\theta_{s\text{-}CO_2r} = \theta^{\circ}_{s\text{-}CO_2r} - \theta^{\circ}_{s\text{-}H}\exp\left(-\vec{k}'_{I\text{-}3}Fc_{CO_2}(\text{sol})t_{ad}/Q^{a}_{s\text{-}H}\right) \tag{11}$$

where $\theta^{\circ}_{s\text{-}H}$ is the value of $\theta_{s\text{-}H}$ for $t_{ad} = 0$ and $\theta^{\circ}_{s\text{-}CO_2r}$ is the value of θ_{CO_2r} for $t_{ad} \to \infty$. However, this type of dependence is not observed for reaction (I-3) except when $t_{ad} \to 0$. In this limiting case one should expect an increase of the initial slope in the θ_{CO_2r} vs. t_{ad} plot with decreasing E_{ad}. This fact is, in principle, obeyed as can be seen through the experimental results in Fig. 2.

Another possibility exists for the case where the rate of diffusion of CO_2 becomes the rate determining step. Then, if the diffusion of CO_2 follows Fick's equation for linear diffusion (x-direction) to a plane electrode, that is [32]:

$$D_{CO_2}\left(\frac{dc_{CO_2}(\text{elec})}{dx}\right)_{x=0} = c_{CO_2}(\text{sol})\left(\frac{D_{CO_2}}{\pi}\right)^{1/2}\frac{1}{t_{ad}^{1/2}} \tag{12}$$

where D_{CO_2} is the diffusion coefficient of CO_2 in the electrolyte solution, the expression for $\vec{v}_{I\text{-}3}$ becomes:

$$\vec{v}_{I\text{-}3} = c_{CO_2}(\text{sol})\left(\frac{D_{CO_2}}{\pi}\right)^{1/2}\frac{1}{t_{ad}^{1/2}} \tag{13}$$

Considering the relation between $\vec{v}_{I\text{-}3}$ and $\theta_{s\text{-}CO_2r}$ already indicated, integration of eqn. (13) at constant E_{ad} yields:

$$\theta_{s\text{-}CO_2r} = \frac{F}{Q^a_{CO_2r}} \frac{c_{CO_2}(sol)}{\pi^{1/2}} D^{1/2}_{CO_2} t^{1/2}_{ad} + \text{const.} \tag{14}$$

The value of $Q^a_{CO_2r}$ depends on E_{ad}, that is, on the initial value of θ_H. Equation (14) predicts a first order dependence on $c_{CO_2}(sol)$, and it is approached by the experimental data at low values of E_{ad}, i.e. for $\theta_H \to 1$, and for relatively small t_{ad} values, so that reaction scheme I predominates, i.e. that involving s-H adatoms.

It is worth noting that an expression similar to eqn. (14) has been derived for the adsorption kinetics of neutral molecules on electrodes [33]. Such an equation is applicable to the present case if one considers that the adsorbate surface concentration is nearly the surface concentration for maximum coverage even for $c_{CO_2}(elec) \ll c_{CO_2}(sol)$, and the rate of diffusion of CO_2 is the same as for a process in which $c_{CO_2}(elec) = 0$ for large t_{ad} and $c_{CO_2}(elec) = c_{CO_2}(sol)$ for $t_{ad} = 0$. This major simplification is justifiable when $c_{CO_2}(sol)$ is so large that the maximum value of $Q^a_{CO_2r}$ at E_{ad} is reached even when $c_{CO_2}(elec)$ is much smaller than $c_{CO_2}(sol)$. Presumably this can be the case when $\theta_H \to 0$, that is, for large positive values of E_{ad}. Then, for the reaction involving the s-H adatoms one obtains [33]:

$$\Gamma_{CO_2r} = \frac{2 D^{1/2}_{CO_2} c_{CO_2}(sol)}{\pi^{1/2}} t^{1/2}_{ad} \tag{15}$$

where Γ_{CO_2r} is the surface concentration of the adsorbate. As the latter appears as the voltammetric electrooxidation charge, for small t_{ad} eqn. (15) explains that, under this particular set of conditions, a linear $Q^a_{CO_2r}$ vs. $t^{1/2}_{ad}$ dependence be approached (Fig. 3), the slope of these straight lines depending on E_{ad}.

Analysis of scheme II

The experimental results obtained by setting E_{ad} at less positive potentials, that is, in the potential range where weakly bound H atoms are produced, indicate that in this case the reduced CO_2 species is oxidized more easily than that formed in the potential range of strongly bound H adatoms. The reaction between w-H adatoms and CO_2 appears to be a rather slow process, as seen for instance in Figs. 5 and 6, so that the adsorption reaction itself would become the rate determining step. In practice, the kinetic analysis developed for scheme I can be applied to scheme II. Thus, an expression of $\vec{v}_{II\text{-}3}$ similar to eqn. (6) can be derived when the w-H adatoms become the adsorbed reactant for reduced CO_2 adsorbate formation at E_{ad}. In this case, the slowness of reaction (II-3) makes it possible that $k_2 \gg \vec{k}'_{II\text{-}3}\theta_{w\text{-}H}$, and $\vec{k}_2 c_{CO_2}(sol) \gg \overleftarrow{k}'_{II\text{-}3}\theta_{w\text{-}CO_2r}$. Then,

$$\vec{v}_{II\text{-}3} = \frac{\vec{k}'_{II\text{-}3}\vec{k}_2}{\overleftarrow{k}_2} c_{CO_2}(sol)\theta_{w\text{-}H} = K_2 \vec{k}'_{II\text{-}3} c_{CO_2}(sol)\theta_{w\text{-}H} \tag{16}$$

Accordingly, eqn. (16) implies a first order dependence of $\vec{v}_{II\text{-}3}$ on CO_2(sol) when $\theta_{w\text{-}H}$ = constant. This situation is approached for small values of t_{ad} and low CO_2 concentration in solution (Figs. 7c and d).

Comparison of kinetic data resulting on different Pt electrodes

The interpretation advanced in the present work for CO_2 adsorption kinetics on H adatom covered electrodispersed Pt electrodes is rather different from that given earlier for smooth and platinized Pt [8,11–13]. Accordingly, the rate of the reaction

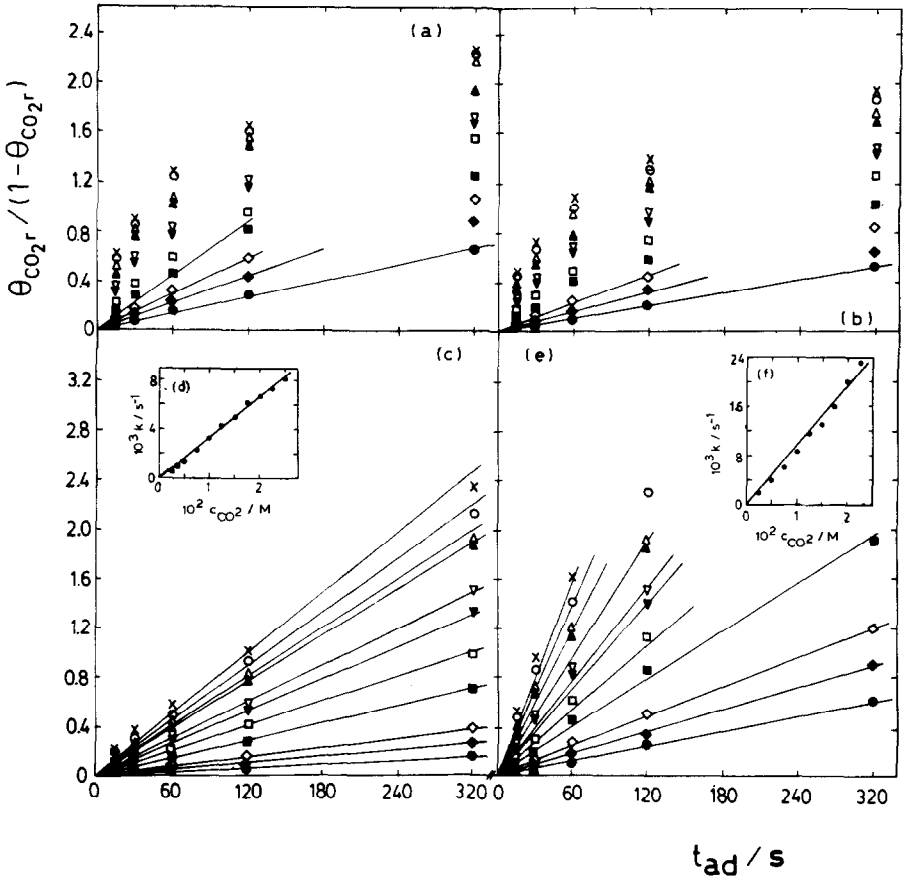

Fig. 8. $\theta_{CO_2r}/(1-\theta_{CO_2r})$ vs. t_{ad} plots (a, b, c and e) for different E_{ad} and CO_2 concentrations in solution. The rate constants (k) calculated from the slopes of the straight line plots are plotted against the CO_2 concentration in solution in the insets (d and f). E_{ad}/V: (a) 0.065, (b) 0.015, (c) 0.165, (e) 0.115. c_{CO_2}/M: (×) 0.025, (○) 0.0225, (△) 0.02, (▲) 0.0175, (▽) 0.015, (▼) 0.0125, (□) 0.01, (■) 0.0075, (◇) 0.005, (◆) 0.0035, (●) 0.0025.

on these electrodes was described by the equation:

$$d\theta/dt = k(1-\theta)^p \quad (17)$$

where k is a formal rate constant and p corresponds to the reaction order. In that work [8,11–13], it was assumed that the concentration of CO_2 was much greater than that of the H adatoms at a constant potential and the value of $(1-\theta)$ was taken as equivalent to the surface concentration of H atoms available for reaction with CO_2. For high H atom concentrations, p was taken equal to 2, so that after integration it followed that $\theta/(1-\theta) = kt$. The present results, plotted as $\theta/(1-\theta)$ vs. t (Fig. 8), yield straight lines only for the most positive values of E_{ad} and the lowest CO_2 concentrations. In these cases the plot of k vs. CO_2 concentration in the solution gives a linear relationship (Figs. 8d and f), which agrees with a first order reaction with respect to CO_2 in solution.

CONCLUSIONS

The kinetics of the electroformation of reduced CO_2 adsorbate on electrodispersed Pt in acid solutions can be explained satisfactorily through a mechanism which can be applied to both strongly and weakly bound adsorbates (s-H and w-H and s-CO_2r and w-CO_2r). Each mechanism involves three steps, namely, the initial equilibrium electroadsorption of H adatoms, the transport of CO_2 from the solution to the interface, and the formation of the reduced CO_2 adsorbate through a reaction between CO_2 and H adatoms. At the highest E_{ad}, where the s-H adatoms predominate, the formation of the s-CO_2r adsorbate involves a slow transport of CO_2 from solution. Under these circumstances a large influence of anions on the H adatom electrosorption reactions can be noted [34,35], although due to the strong influence of diffusional processes on the kinetics of the reaction, the influence of the electrolyte composition on the entire process of reduced CO_2 electroformation becomes relatively small. The formation of w-CO_2r adsorbate appears to be determined by adsorption kinetics. The reaction between w-H atoms and CO_2 becomes a rather slow process.

Further aspects of the reaction mechanisms, including possible interconversion processes and adsorbate structures, will be discussed in a future publication based upon the temperature dependence of the kinetics of the reactions.

ACKNOWLEDGEMENTS

This work was partially supported by the Regional Program for the Scientific and Technological Development of the Organization of the American States. The authots thank the D.G.C. y T. (Spain) for financial support of the present work.

REFERENCES

1 P.G. Russell, N. Kovac, S. Srinivasan and M. Steinberg, J. Electrochem. Soc., 124 (1977) 1329.
2 U. Kaiser and E. Heitz, Ber. Bunsenges. Phys. Chem., 77 (1973) 818.

3 K. Ogura and M. Takagi, J. Electroanal. Chem., 201 (1986) 359; 206 (1986) 209.
4 J. Giner, Electrochim. Acta, 8 (1963) 857; 9 (1964) 63.
5 B.J. Piersma, T.B. Warner and S. Schuldiner, J. Electrochem. Soc., 113 (1966) 841.
6 M.W. Breiter, Electrochim. Acta, 12 (1967) 1213.
7 M.W. Breiter, J. Electroanal. Chem., 19 (1968) 131; B. Beden, A. Bewick, M. Razaq and J. Weber, J. Electroanal. Chem., 139 (1982) 203.
8 S.B. Brummer and K. Cahill, J. Electroanal. Chem., 21 (1969) 463.
9 B.E. Kazarinov, N.V. Andreev and G.J. Tysiacznaja, Elektrokhimiya, 8 (1972) 927.
10 N.B. Urbach, I.G. Adams and R.E. Smith, J. Electrochem. Soc., 121 (1974) 233.
11 J. Sobkowski and A. Czerwinski, J. Electroanal. Chem., 55 (1974) 391.
12 A. Czerwinski and J. Sobkowski, J. Electroanal. Chem., 59 (1975) 41.
13 J. Sobkowski and A. Czerwinski, J. Electroanal. Chem., 65 (1975) 327.
14 A.V. Zakharyan, N.V. Osetrova and Yu.B. Vasiliev, Elektrokhimiya, 12 (1976) 1854.
15 N.V. Andreev, Yu.B. Vasiliev, N.V. Osetrova and T.N. Yastrebova, Elektrokhimiya, 13 (1983) 381.
16 A.A. Mikhailova, N.V. Osetrova and Yu.B. Vasiliev, Elektrokhimiya, 21 (1985) 1051.
17 A.M. Baruzzi, E.P.M. Leiva and M.C. Giordano, J. Electroanal. Chem., 158 (1983) 103.
18 A.M. Baruzzi, E.P.M. Leiva and M.C. Giordano, J. Electroanal. Chem., 189 (1985) 257.
19 N.A. Maiorova, A.A. Mikhailova, O.A. Khazova and Yu.B. Vasiliev, Elektrokhimiya, 22 (1986) 96.
20 C. Alonso, J. González-Velasco and A.J. Arvia, J. Electroanal. Chem., 250 (1988) 183.
21 M.L. Marcos, J. González-Velasco, J.M. Vara and A.J. Arvia, J. Electroanal. Chem., 224 (1987) 189.
22 M.L. Marcos, J. González-Velasco, J.M. Vara, M.C. Giordano and A.J. Arvia, J. Electroanal. Chem., 270 (1989) 205.
23 L. Vázquez, J. Gómez, A.M. Baró, M.L. Marcos, J. González-Velasco, J.M. Vara, A.J. Arvia, J. Presa, A. García and M. Aguilar, J. Am. Chem. Soc., 109 (1987) 1730.
24 L. Vázquez, A. Bartolomé, A.M. Baró, C. Alonso, R.C. Salvarezza and A.J. Arvia, Surf. Sci., 215 (1989) 171.
25 A.C. Chialvo, W.E. Triaca and A.J. Arvia, J. Electroanal. Chem., 146 (1983) 93.
26 E.W. Washburn (Ed.), International Critical Tables, Vol. 3, McGraw-Hill, New York, London, 1928, pp. 260, 276.
27 F.G. Will and C.A. Knorr, Z. Elektrochem., 64 (1960) 258.
28 K. Yamamoto, D.M. Kolb, R. Kötz and G. Lehmpfuhl, J. Electroanal. Chem., 96 (1979) 233.
29 G.N. Salaita, F. Lu, L. Laguren-Davidson and A.T. Hubbard, J. Electroanal. Chem., 229 (1987) 1.
30 D. Aberdam, R. Durand, R. Faure and F. El-Omar, Surf. Sci., 171 (1986) 303.
31 A.U. Tripkovic and R.R. Adzic, J. Electroanal. Chem., 205 (1986) 335.
32 P. Delahay, New Instrumental Methods in Electrochemistry, 3rd ed., Interscience, New York, 1962, p. 51.
33 P. Delahay and I. Trachtenberg, J. Am. Chem. Soc., 79 (1977) 2355.
34 J.C. Huang, W.E. O'Grady and E. Yeager, J. Electrochem. Soc., 124 (1977) 1732.
35 S.A. Bilmes, M.C. Giordano and A.J. Arvia, Can. J. Chem., 66 (1988) 2259.